Modulation of hyaluronan synthases and involvement of T cell-derived hyaluronan in autoimmune responses to transplanted islets

John A. Gebe [a], Michel D. Gooden [a], Gail Workman [a], Nadine Nagy [b], Paul L. Bollyky [b], Thomas N. Wight [a] and Robert B. Vernon [a]

a - Center for Fundamental Immunology, *Matrix Biology Program, Benaroya Research Institute at Virginia Mason, Seattle, WA, USA*
b - Division of Infectious Diseases and Geographic Medicine, *Department of Medicine, Stanford University School of Medicine, Stanford, CA, USA*

Correspondence to Robert B. Vernon:*at: Center for Fundamental Immunology, Benaroya Research Institute at Virginia Mason, 1201 Ninth Avenue, Seattle, WA 98101, USA. rvernon@benaroyaresearch.org*
https://doi.org/10.1016/j.mbplus.2020.100052

Abstract

The extracellular matrix glycosaminoglycan hyaluronan (HA) accumulates in human and mouse islets during the onset of autoimmune type 1 diabetes (T1D). HA plays a critical role in T1D pathogenesis, as spontaneous disease is blocked in mice fed the HA synthesis inhibitor 4-methylumbelliferone (4MU). The present study demonstrates the involvement of HA in T cell-mediated autoimmune responses to transplanted islets and in in vivo and in vitro T cell activation. Scaffolded islet implants (SIs) loaded with RIP-mOVA mouse islets expressing chicken ovalbumin (OVA) on their β cells were grafted into T and B cell-deficient RIP-mOVA mice, which subsequently received $CD4^+$ T cells from DO11.10 transgenic mice bearing OVA peptide-specific T cell receptors (TcRs), followed by injection of OVA peptide to induce an immune response to the OVA-expressing islets. By affinity histochemistry (AHC), HA was greatly increased in grafted islets with T cell infiltrates (compared to islets grafted into mice lacking T cells) and a portion of this HA co-localized with the infiltrating T cells. Transferred T cells underwent HA synthase (HAS) isoform switching – T cells isolated from the SI grafts strongly upregulated HAS1 and HAS2 mRNAs and downregulated HAS3 mRNA, in contrast to T cells from graft-draining mesenteric lymph nodes, which expressed HAS3 mRNA only. Expression of HAS1 and HAS2 proteins by T cells in SI infiltrates was confirmed by immunohistochemistry (IHC). DO11.10 mice fed 4MU had suppressed in vivo T cell immune priming (measured as a reduced recall response to OVA peptide) compared to T cells from control mice fed a normal diet. In co-cultures of naïve DO11.10 T cells and OVA peptide-loaded antigen-presenting cells (APCs), pre-exposure of the T cells (but not pre-exposure of APCs) to 4MU inhibited early T cell activation (CD69 expression). In addition, T cells exposed to 4MU during activation in vitro with anti-CD3/CD28 antibodies had inhibited phosphorylation of the CD3ζ subunit of the TcR, a very early event in TcR signaling. Collectively, our results demonstrate that T cell-derived HA plays a significant role in T cell immune responses, and that expression of T cell HAS isoforms changes in a locale-specific manner during in vivo priming and functional phases of the T cell response.

Introduction

The glycosaminoglycan *hyaluronan (HA)* is a long, non-branching polymer made up of repeating disaccharides of *N*-acetylglucosamine and glucuronic acid. HA is an important structural component of the extracellular matrix of many tissues. HA regulates tissue hydration and osmotic balance in extracellular compartments [1] and serves as a scaffold for support of HA-binding proteins and proteoglycans *(hyaladherins)* [2], which interact with HA to form supramolecular assemblies that exert a variety of biological effects [3–5].

In addition to its structural role, HA interacts with cells via receptor-mediated signaling to regulate a variety of cell behaviors (e.g., proliferation, motility,

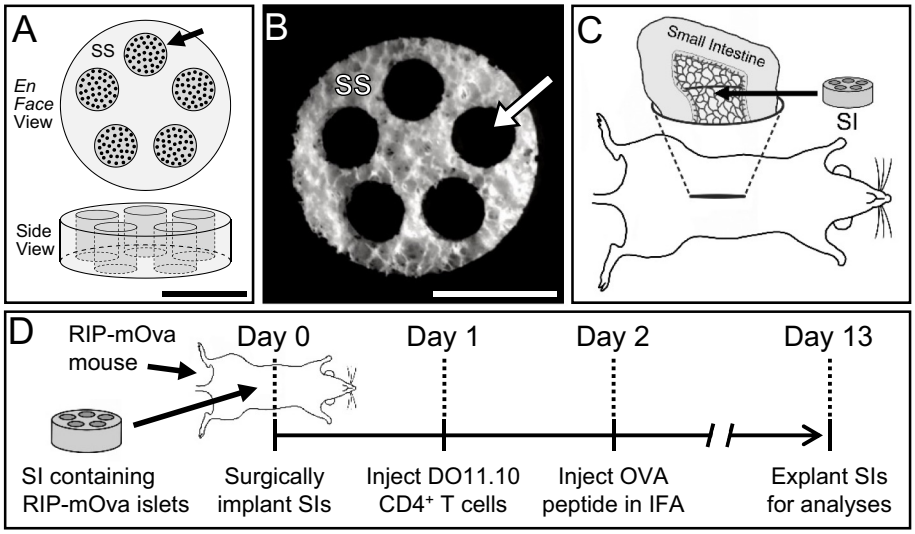

Fig. 1. A) Diagram of SI design. *En face* view shows the 8-mm diameter PVA sponge scaffold (SS – light gray) with five, 2-mm diameter chambers (e.g., arrow), each filled with collagen hydrogel (dark gray) containing suspended islets (black dots). Side view shows cylindrical shape of the chambers and collagen gels (dark gray) within the sponge scaffold (light gray). Islets are omitted for clarity. B) Photo of sponge scaffold (SS). Arrow indicates a chamber. C) Diagram illustrating placement of the SI in a mesenteric pocket. D) Summary of the RIP-mOVA/DO11.10 T cell transfer model of T1D autoimmunity. IFA = incomplete Freund's adjuvant. Scale bars in A and B = 4 mm.

adhesion) involved in such processes as angiogenesis, wound repair, tumor metastasis, and inflammation [4,6,7]. HA is made by *hyaluronan synthases (HASes)* which, in mammals, exist in three isoforms (HAS1, -2, and -3) [8]. In healthy tissues, HA is present in high molecular weight forms (> ~1000 kDa) which have anti-inflammatory properties [7,9]; however, during inflammation or infection, HA is degraded by hyaluronidases, mechanical forces, and oxidation [10,11] into fragments of lower molecular weight (< 500–700 kDa), which are considered to be generally pro-inflammatory [4,7,12,13].

There is increasing evidence that HA is involved in immune dysfunction, which includes a spectrum of autoimmune diseases, including type 1 diabetes (T1D) [14]. In normally-functioning human and mouse pancreatic islets, HA is found in basement membranes of peri-islet and intra-islet vasculature [15–17]. However, during the development of T1D in humans and in mice that model this autoimmune disease (e.g., non-obese diabetic [NOD] and DO11.10 x RIP-mOVA [DORmO] mice), there is a substantial increase in HA around peri- and intra-islet microvessels and accumulation of HA in leukocytic infiltrates [16–18]. The cellular source of the increased HA is largely unknown. Remarkably, dietary administration of an inhibitor of HA synthesis, 4-methylumbelliferone (4MU), to NOD or DORmO mice halts the progression of diabetes even after the onset of insulitis [18], pointing to a critical role for HA as a mediator of autoimmunity in the setting of T1D.

Immune-mediated rejection is of critical concern in islet transplantation therapies to replace pancreatic islets lost during T1D progression. Islet transplant patients typically receive lifelong immunosuppressive drugs, which are effective at controlling acute post-transplantation rejection; however, transplants can be lost from later-term allorejection and reoccurring autoimmunity (i.e., a lack of durable tolerance to the graft) [19–21]. In the context of islet replacement therapy, we have developed *scaffolded islet implant (SI)* test-beds to evaluate strategies to improve survival and function of transplanted islets in non-hepatic (mesenteric or subcutaneous) graft sites. The SIs consist of a disk-shaped, polyvinyl alcohol (PVA) sponge scaffold with collagen gel-filled chambers that retain the islets. SIs loaded with 400–500 syngeneic islets and implanted on the gut mesentery of mice with streptozotocin-induced diabetes (one SI per mouse) became vascularized within 1–2 weeks and reversed diabetes in experiments lasting 54 days [22] to over 200 days (unpublished data). Our recent studies have demonstrated that controlled release of vascular endothelial growth factor [23] and immunomodulatory monoclonal antibodies (mAbs) [24] within SIs have beneficial effects on the survival and function of transplanted islets.

The present study combines SIs with a mouse model of T1D to evaluate the involvement of HA in the rejection of transplanted islets. Here, we focus on the T cell – the cell type central to autoimmune responses. Like many cell types, T cells can synthesize HA [25,26], but the function of T cell-derived HA has received relatively little attention. The results of our study demonstrate: 1) a significant

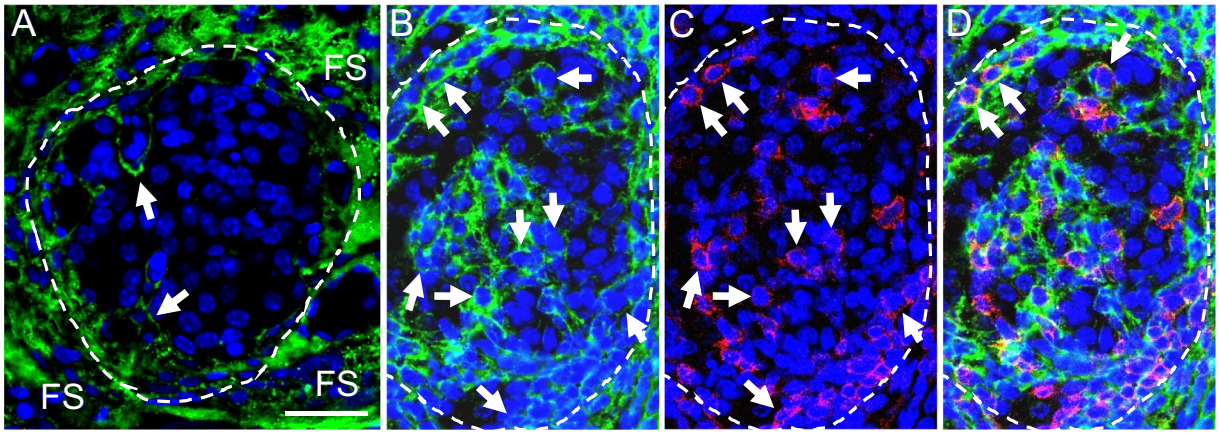

Fig. 2. Association of HA with T cells invading transplanted islets. RIP-mOVA islets in SIs were implanted into RIP-mOVA mice. After 13 days, the SIs were explanted, FFPE/sectioned, and stained for HA (green) and T cell-associated CD3 (red). Nuclei were stained with DAPI (blue). A) An islet (dashed outline) implanted in a control mouse that did not receive DO11.10 T cells and OVA peptide priming has no CD3 staining and only a small amount of HA associated with interior microvessels (arrows). The islet is surrounded by HA of host-derived fibrovascular stroma (FS). B, C) Single islet (dashed outline) in a mouse that received DO11.10 T cells and OVA peptide priming contains high levels of cell-associated HA (B). Many of the HA-positive cells also show a punctate expression of CD3 (C) – examples of double-stained cells are indicated by arrows in B and C. A merge of B and C (D) shows areas of yellow (e.g., arrows) where the HA and CD3 signals of T cells are mutually strong and closely overlapped. A–D are equal magnifications. Scale bar in A = 50 μm.

and unexpected modulation of HAS isoform expression in T cells during the immune response to transplanted islets, and 2) that suppression of HA synthesis in T cells suppresses early events in the T cell receptor (TcR) activation cascade and immune priming that occur during engagement of T cells with antigen-presenting cells (APCs).

Results

Islet transplantation experiments were conducted using SIs with disk-shaped PVA sponge scaffolds of 8 mm diameter and 2 mm thickness. Each scaffold incorporated five cylindrical chambers (each 2 mm in diameter and 2 mm deep) which were filled with type I collagen hydrogel containing suspended islets (Fig. 1A–C). The SIs were used in conjunction with the RIP-mOVA/DO11.10 T cell transfer model of T1D autoimmunity [27] (Fig. 1D). In this model, $CD4^+$ T cells from transgenic DO11.10/$Rag2^{-/-}$ mice, which have TcRs that recognize amino acids 323–339 within chicken ovalbumin (OVA), are infused intravenously into RIP-mOVA/$Rag2^{-/-}$ (RIP-mOVA) mice, which lack endogenous T and B cells and express a membrane-bound form of OVA (mOVA) on islet β cells, driven by the rat insulin promoter (RIP) [28]. Subsequent to the T cell infusion, the mice are injected with $OVA_{323–339}$ peptide, which stimulates (primes) the immune system, activating the T cells to attack islet β cells in the pancreas. If these mice are transplanted with SIs containing RIP-mOVA islets, as in the present study, the activated T cells will also attack the β cells in the transplant. Experiments using this model are described below.

Thirteen days after SI grafting (11 days after OVA peptide priming) the grafted mice had become hyperglycemic due to autoimmune destruction of their native and transplanted islets. At this point, the SIs were explanted, formalin-fixed/paraffin-embedded (FFPE), thin-sectioned, and subjected to affinity histochemistry (AHC) to detect HA, using purified HA-binding protein (HABP). The sections were also labeled by immunohistochemistry (IHC) for CD3 (a component of the TcR) to identify T cells that had migrated into the SIs. AHC detected a small amount of HA within transplanted islets from mice that did not receive T cells and priming with OVA peptide. This HA was associated with islet microvessels (Fig. 2A). In contrast, there was a substantial accumulation of HA within islets transplanted into mice that had received T cells and OVA peptide priming (Fig. 2B). These islets contained T cells, as indicated by punctate staining for CD3 (Fig. 2C). A substantial proportion of these T cells had HA in close proximity to the cell (Fig. 2B–D).

AHC alone did not indicate whether the T cell-associated HA was a product of the T cells themselves, or might have come from other cell sources. In this context, we showed that activated DO11.10 T cells cultured for 4 days in the absence of other cell types could express HA on their surfaces (Fig. 3A), which could be removed by

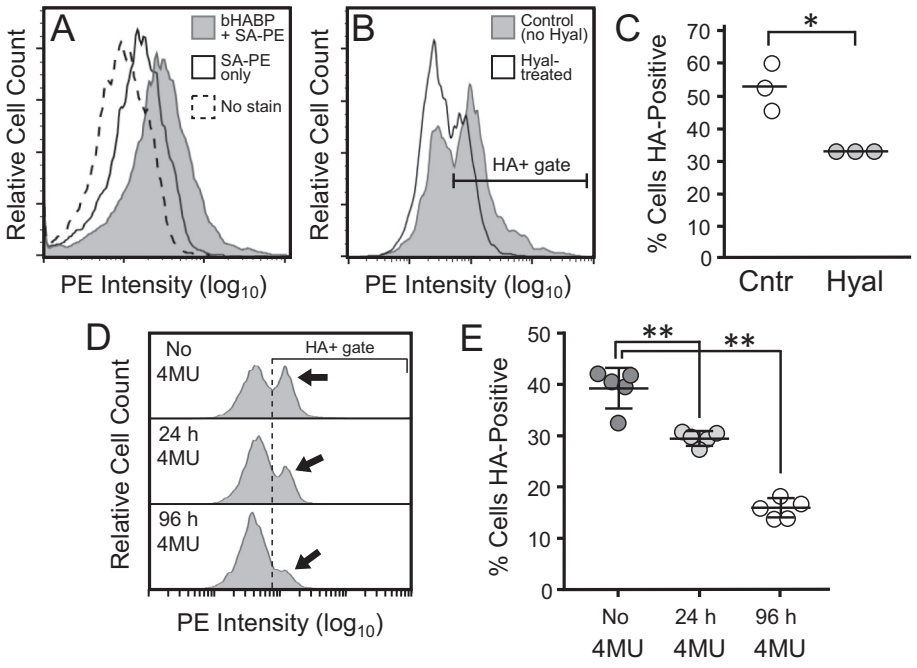

Fig. 3. HA is present on the T cell surface. A–E) $CD4^+$ T cells isolated from DO11.10 mice were cultured 3–4 days with anti-CD3/CD28 mAbs and then stained for surface HA using bHABP and streptavidin-phycoerythrin (SA-PE), followed by analysis by flow cytometry. A) Plot shows substantial increase in HA signal of 4-day-cultured T cells stained with bHABP + SA-PE vs. controls stained with SA-PE only or not stained. B) T cells cultured 3 days, then exposed to 20 U/mL of hyaluronidase (Hyal) for 2 h at 37 °C showed a significant reduction of HA signal compared to untreated controls. Bar ("HA + gate") indicates cells scored as HA-positive. C) Percentage of HA+ cells within control vs. Hyal-treated T cell populations in 3 replicate experiments, conducted as described in "B". $^*P < 0.01$. D) T cells cultured 4 days with 100 µg/mL of 4MU present continuously (96 h), present on day 3–4 only (24 h), or not added to the cultures (No 4MU). Numbers of HA+ T cells diminished with increased exposure time to 4MU (arrows). E) Percentage of HA+ cells within control vs. 4MU-treated T cell populations in 5 replicate experiments, conducted as described in "D". $^{**}P < 0.001$.

treatment with hyaluronidase (Fig. 3B, C). Moreover, a graded increase in exposure of cultured, activated T cells to the HA synthesis inhibitor 4MU corresponded to a graded reduction in expression of surface HA on the cells (Fig. 3D, E).

In subsequent experiments in vivo, we assayed for HAS1–3 mRNAs in $CD3^+/CD4^+$ T cells isolated from SIs explanted from RIP-mOVA mice 16 days after grafting. As a comparison, we measured these mRNAs in $CD3^+/CD4^+$ T cells from the mesenteric lymph nodes (MLNs) draining the SI grafts. T cells that had infiltrated the SIs expressed high levels (for HASes) of HAS1 mRNA (avg. copy number [CN] of 452.0; Fig. 4A), but substantially lower levels of HAS2 mRNA (avg. CN of 33.1; Fig. 4B). HAS3 mRNA expression was negligible (avg. CN of 0.33; Fig. 4C). In contrast, HAS1 and -2 mRNAs were not expressed by T cells from the MLNs (Fig. 4A, B), but HAS3 mRNA was detectable, albeit at low levels (avg. CN of 5.4; Fig. 4C). IHC performed on FFPE/sectioned SIs bearing islets confirmed HAS1 and -2 protein expression by $CD3^+$ T cells infiltrating the SIs (Fig. 4D–I). In contrast to the HAS mRNAs, the expression of mRNAs for the HA-degrading enzymes hyaluronidase 1 and -2 (Fig. 4J, K) was either undetectable or uniformly very low (for hyaluronidases) in T cells from SIs and MLNs. When mRNA levels of each hyaluronidase isoform were compared in T cells from SIs vs. MLNs, no significant differences in expression were observed.

Dietary administration of 4MU halts the progression of diabetes in NOD and DORmO mice [18] by mechanisms that are not fully understood. As T cell priming (i.e., the initial activation of naïve T cells by antigen) is central to immune responses, we examined the effect of 4MU on T cell priming in vivo. DO11.10 mice were fed a diet containing 4MU for two weeks, then primed by a subcutaneous injection of OVA peptide and subsequently switched to a control diet lacking 4MU to remove the 4MU from the environment (4MU has a short half-life in vivo [~5 h]), the intent being to limit the influence of the 4MU to the initial priming events and avoid the potential for off-target effects of the 4MU on downstream behaviors (e.g., proliferation/survival) by the activated T cells. A group of control mice were fed only the control diet for the entire duration of the experiment. Two weeks after OVA priming, T cells were isolated from the inguinal lymph nodes (ILNs) that drained the injection site and evaluated for a

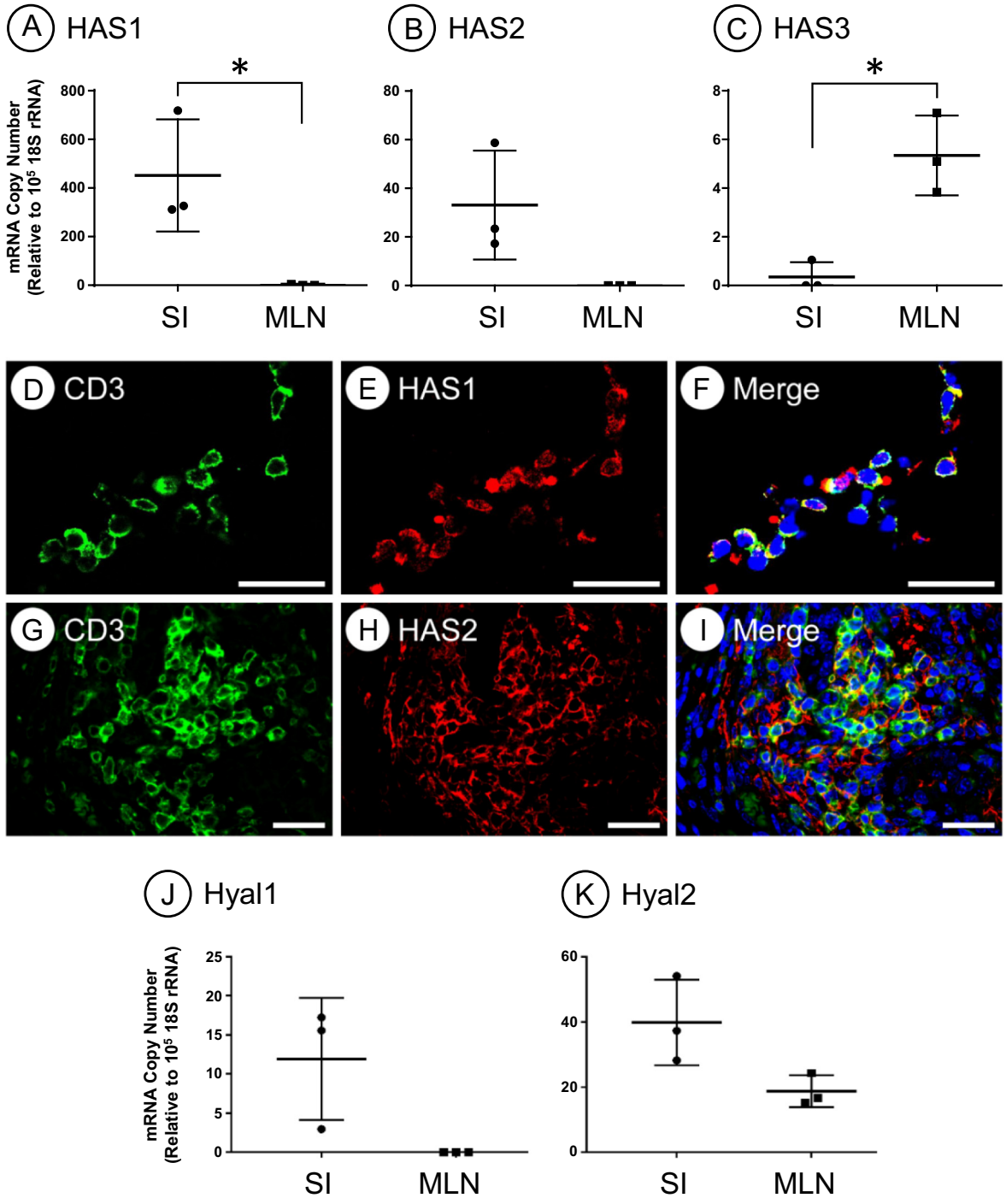

Fig. 4. A–C) Expression of T cell HAS and hyaluronidase (Hyal) mRNAs in SIs vs. MLNs. SIs containing RIP-mOVA islets were implanted into RIP-mOVA mice, followed by T cell transfer and OVA priming. Sixteen days after grafting, the SIs and MLNs were removed, the $CD3^+/CD4^+$ T cells were isolated, and mRNA measured. T cells that infiltrated SIs expressed high levels of HAS1 mRNA (A), substantially lower levels of HAS2 mRNA (B), and negligible HAS3 mRNA (C). In contrast, HAS1 and -2 mRNAs were not expressed by MLN T cells, but HAS3 mRNA was expressed at low levels. $^*P < 0.05$. $n = 3$ mice. D–I) SIs like those in A–C were explanted, FFPE/sectioned, and stained by IHC for CD3 and HAS1 and -2 proteins. $CD3^+$ T cells within the SI (D, green) express HAS1 (E, red). D-E merge shows co-localization of CD3 and HAS1 (F, yellow). $CD3^+$ T cells also express HAS2 (G, H), with the merged image showing co-localization (I, yellow). In F and I, cell nuclei are stained with DAPI (blue). Scale bars in D–I = 50 μm. T cells isolated from SIs and MLNs like those in A–C had levels of Hyal1 (J) and Hyal2 (K) mRNAs that were low or undetectable. $n = 3$ mice.

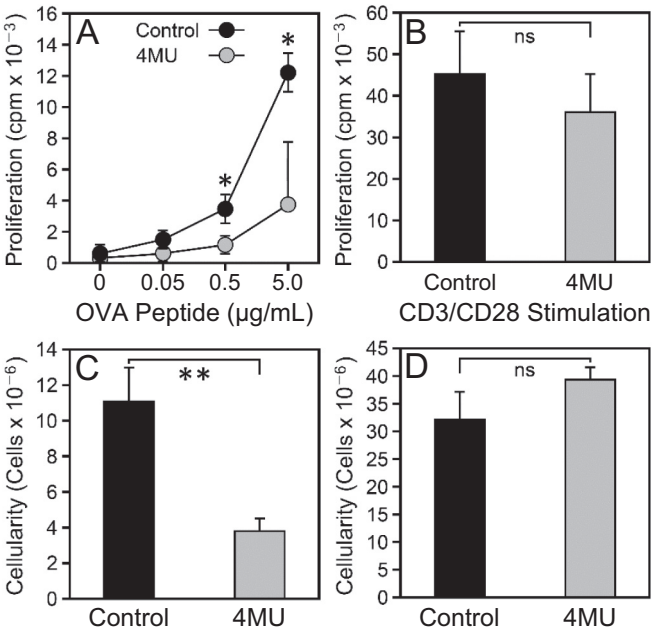

Fig. 5. Short-term dietary 4MU decreases priming of T cells in vivo. DO11.10 mice were fed a diet containing 5% 4MU for 2 weeks or a control diet lacking 4MU. Subsequently, both groups of mice received a normal diet and were injected with OVA peptide. Two weeks later, T cells from the ILNs were isolated and assayed for proliferation in response to graded OVA peptide exposure in vitro. Compared to T cells from the control mice, ILN T cells from the 4MU-fed mice exhibited significantly suppressed proliferation (A). T cells from both groups of mice responded similarly in vitro to strong stimulation with anti-CD3/CD28 mAbs (B). Reduced T cell priming in the 4MU-fed mice relative to the control mice was correlated with lower immune cell numbers (cellularity) in ILNs (C), but not spleens (D). $^{*}P < 0.05$, $^{**}P < 0.01$. $n = 3$ mice in each group.

recall (proliferative) response to graded concentrations of OVA peptide in vitro. Consistent with a suppressive effect of 4MU exposure on T cell priming, the recall response of the ILN T cells from the 4MU-fed mice was significantly lower than the response of corresponding T cells from the control mice (Fig. 5A). Proliferation in vitro in response to strong stimulation by anti-CD3/CD28 mAbs was not significantly different between the 4MU and control groups of T cells (Fig. 5B), indicating that 4MU did not inhibit the intrinsic capacity of T cells to divide. Inhibition of priming by 4MU was also indicated by a significantly reduced number of immune cells in the ILNs (i.e., reduced ILN cellularity) of the 4MU-fed mice relative to control mice (Fig. 5C), indicating a 4MU-mediated suppression of T cell proliferation in vivo in response to OVA peptide. 4MU-mediated reductions in ILN cellularity did not indicate systemic lymphopenia (e.g., as a result of a toxic effect of 4MU on T cells), as the cellularity of the spleens of the 4MU-fed and control mice was not significantly different (Fig. 5D).

As T cell priming involves interaction of T cells with APCs, we sought to determine the relative effect of inhibition of HA synthesis by T cells vs. APCs on the priming event. Experiments were performed in vitro. Purified naïve DO11.10 $CD4^+$ T cells and adherent APCs were separately cultured for 24 h in the presence of 0, 20, 50, or 100 μg/mL of 4MU, then washed, combined, and co-cultured for 24 h in the presence of OVA peptide. Subsequently, the T cells were assayed for priming by flow cytometry for expression of the early activation cell surface marker CD69. As a positive control, we observed that in the absence of 4MU pre-exposure, addition of OVA peptide to co-cultures resulted in a characteristic CD69 upregulation by the T cells, compared to co-cultures not exposed to the peptide (Fig. 6A). OVA peptide-induced CD69 upregulation by T cells within the co-cultures was inhibited when the T cells were pre-exposed to 4MU (Fig. 6B, C). This inhibition was dose-dependent – pre-exposure of the T cells to increasing concentrations of 4MU resulted in decreasing expression of CD69 (Fig. 6B). In contrast, CD69 upregulation by T cells was not inhibited when the APCs were pre-exposed to 4MU (Fig. 6B, C).

Having shown that expression of CD69 was influenced by T cell-derived HA, we examined whether T cell-derived HA might be involved in earlier signaling events in T cells. Accordingly, we evaluated the effect of 4MU on phosphorylation of the CD3ζ subunit of the TcR (CD247), which can be measured in vitro within a few minutes to an hour after engagement of the TcR with ligand [29]. For these experiments, we cultured purified, naïve DO11.10 $CD4^+$ T cells of confirmed viability (Fig. 7A) in medium with or without 100 μg/mL of 4MU for 20 h, followed by direct stimulation of the TcR complex with anti-CD3/CD28 mAbs, which provide stimulation of sufficient strength for CD3ζ phosphorylation to be measured by flow cytometry [29]. We found that in the absence of 4MU, CD3ζ phosphorylation could be measured within 5 min of anti-CD3/CD28 mAb exposure (Fig. 7B). This phosphorylation was inhibited by 4MU (Fig. 7B, C). Collectively, the results from the CD69 expression and CD3ζ phosphorylation experiments underscored the importance of T cell-associated HA in the T cell activation process.

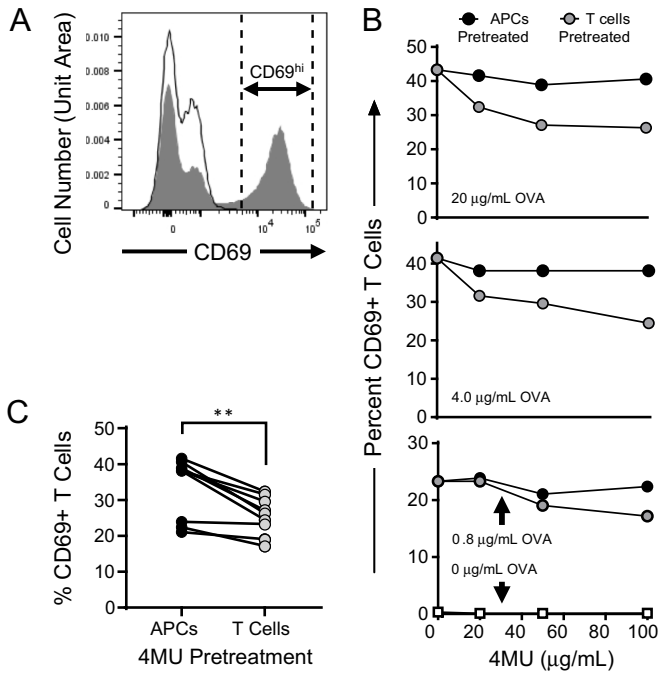

Fig. 6. Pre-exposure of T cells to 4MU in vitro inhibits T cell activation by APCs. Purified naïve DO11.10 CD4$^+$ T cells or adherent APCs were separately cultured (pretreated) for 24 h in the presence of 0, 20, 50, or 100 µg/mL of 4MU, then combined and co-cultured for 24 h with OVA peptide. Subsequently, the T cells were assayed by flow cytometry for CD69 expression. A) In the absence of 4MU pretreatment, co-cultures receiving 20 µg/mL of OVA peptide had substantially higher CD69 expression by the T cells (filled plot, CD69^{hi}) vs. co-cultures not exposed to the peptide (open plot). B) Pretreatment of T cells (gray circles) with increasing concentrations of 4MU suppressed CD69 expression by the T cells when the co-cultures were exposed to OVA peptide at 20, 4.0, or 0.8 µg/mL (top, middle, bottom panels). CD69 expression by T cells was not suppressed when the APCs were pretreated with 4MU (black circles). T cells did not express CD69 in the absence of OVA peptide (bottom panel, white squares). C) Results from "B" expressed as a composite of change in CD69 expression over all OVA peptide and 4MU concentrations. **Equal paired *t*-test, $P < 0.005$. $n =$ 9 mice in each group.

4MU-mediated inhibition of diabetes in mice is associated with suppressed penetration of pancreatic islets by immune cells [18]. Based on this observation and our finding that 4MU suppresses T cell activation, we asked whether dietary administration of 4MU might influence T cell infiltration into SIs. To determine if there was a differential effect of 4MU on T cells vs. other leukocytes (B cells, neutrophils), these studies were performed using mice with fully intact immune systems in an allotransplant setting (i.e., islets from BALB/c donor mice transplanted into C57BL/6 host mice). The C57BL/6 hosts were fed the control or 4MU-supplemented diets for 6 weeks prior to receiving BALB/c donor islets in SIs. Seven days after transplantation (the time when the rejection of the transplanted islets by the host was well underway), the SIs were explanted, FFPE/sectioned, and analyzed by quantitative IHC to assess levels of leukocyte penetration. The analysis revealed no significant differences in the numbers of neutrophils or B cells

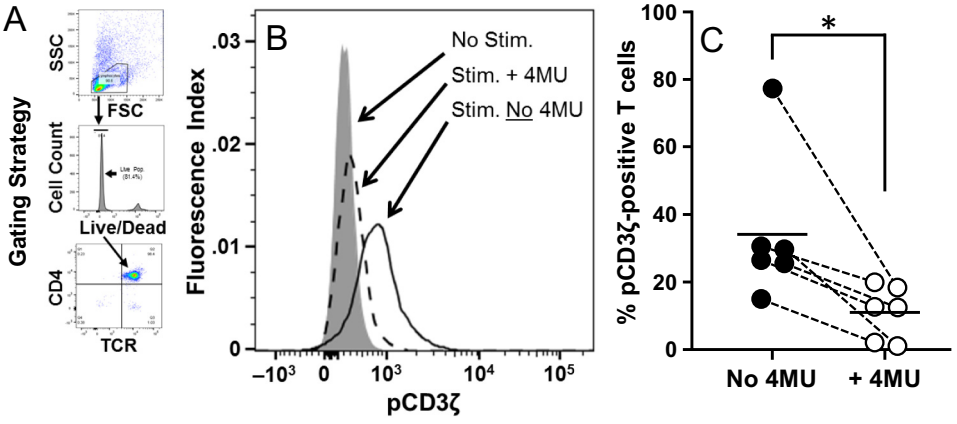

Fig. 7. Pre-exposure of T cells to 4MU in vitro inhibits early signaling in the TcR. Purified naïve DO11.10 CD4$^+$ T cells were separately cultured for 20 h with or without 100 µg/mL of 4MU, washed, allowed to rest for 1 h in 4MU-free medium and then stimulated for 5 min with anti-CD3/CD28 mAbs (2/0.4 µg/mL, respectively). Stimulation was immediately followed by fixation and analysis by flow cytometry for expression of CD4 and phospho- (p)CD3ζ. A) Gating strategy to identify live CD4$^+$ T cells used for pCD3ζ quantitation. B) Expression of pCD3ζ under no mAb stimulation (gray plot), mAb stimulation after 4MU treatment (dashed-line plot), or mAb stimulation without 4MU treatment (solid-line plot) showing inhibition of CD3ζ phosphorylation by 4MU. C) Graph of $n = 6$ experiments showing overall 4MU inhibition of the CD3ζ phosphorylation induced by anti-CD3/CD28 mAb stimulation. *Equal paired *t*-test, $P < 0.04$.

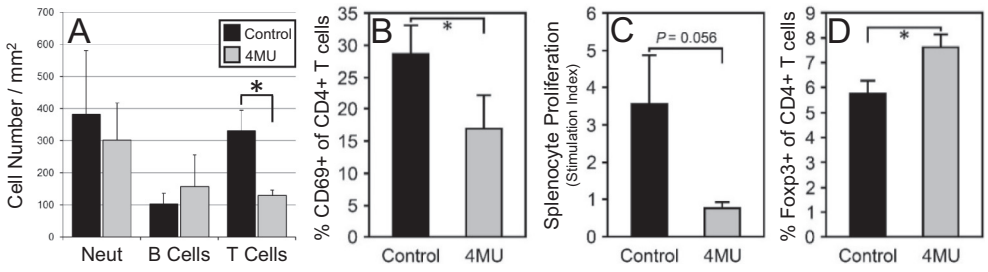

Fig. 8. 4MU inhibits T cell activation and infiltration of SIs. A) C57BL/6 mice were fed a diet containing 5% 4MU for 6 weeks or a diet lacking 4MU (controls). Subsequently, both groups of mice received BALB/c islets in SIs. After 7 days, the SIs were explanted, sectioned, and the infiltrating neutrophils (Neut), B cells, and T cells quantitated by IHC. $*P < 0.03$. $n = 3$ mice per group. B) Similar experiment to "A", but SIs were explanted at 14 days and the infiltrates isolated and analyzed by flow cytometry for CD69 expression. Proliferation of splenocytes from these mice was measured in allo-MLR assays (C) and $CD4^+/CD25^+$ T cells from MLNs were analyzed for Foxp3 expression by flow cytometry (D). In B and D, $*P < 0.05$. $n = 3$ mice per group.

within SIs from the 4MU-fed vs. control mice. However, SIs from the 4MU-fed mice had significantly (> 2.5-fold) lower numbers of T cells relative to the control mice (Fig. 8A). Moreover, flow cytometry showed that T cells isolated from SI allografts explanted from 4MU-fed mice had a significantly lower level of activation (CD69 expression) than did corresponding T cells from the control mice (Fig. 8B). This difference in activation corresponded to a lower proliferative response ($P = 0.056$) by splenocytes from the 4MU-fed mice vs. those from the control mice in allo-mixed lymphocyte reaction (MLR) assays (Fig. 8C). Moreover, there was a significantly higher proportion of $CD4^+/CD25^+/Foxp3^+$ regulatory T cells among the T cells isolated from MLNs from the 4MU-fed mice vs. the control mice (Fig. 8D).

Discussion

With the onset of T1D in humans and mice, there is a substantial accumulation of HA in association with the leukocytes that infiltrate the pancreatic islets, as shown by IHC [16–18]. Although these studies clearly show quantitative increases in intra-islet HA as T1D develops, the source(s) of this HA remain unclear. In the present study, we demonstrated that T1D immune responses elicit an accumulation of HA within transplanted islets that resembles HA deposition in native pancreatic islets. At least a portion of this newly-deposited intra-islet HA is directly associated with infiltrating T cells as shown by AHC/IHC, although histochemical staining alone does not allow us to discern whether the T cells are the source of this HA, or have merely bound and/or internalized HA produced by other cell types.

Activated T cells bind exogenous HA via CD44 [13], but there is also evidence that T cells synthesize HA. Mummert et al. [25] showed, in vitro, that: 1) mRNAs for HASes 1–3 were expressed by both non-activated and concanavalin A (ConA)-activated murine splenic $CD3^+$ T cells, 2) HA was detectable on the surfaces of ConA-activated (but not naïve) T cells, and 3) HA-binding moieties, such as Pep-1 and HABP, blocked the capability of ConA or anti-CD3/CD28 mAbs to stimulate T cell proliferation in the absence of antigen presentation by APCs. There is additional evidence the HA produced by T cells under mitogen stimulation has a direct effect on the T cells themselves, promoting the autocrine production of interleukin (IL)-2 that, in turn, mediates proliferation [26].

In the context of autologous production of HA by T cells, the present study showed that activated DO11.10 T cells cultured for an extended period in the absence of other cell types expressed HA on their surfaces – expression which could be inhibited by 4MU. Of note, DO11.10 T cells isolated from SI grafts expressed HAS1 mRNA at very high levels (for HASes). HAS2 mRNA was expressed at a substantially lower (but potentially biologically significant) level, but HAS3 mRNA expression was negligible. These results were in sharp contrast to HAS mRNA profiles of T cells from MLNs, where HAS3 mRNA was expressed at low levels, but HAS1 and HAS2 mRNAs were not detected. This profile of HAS mRNA expression by $CD4^+$ T cells from MLNs resembles that reported by others for mouse LN and splenic $CD4^+$ T cells activated in vitro by anti-CD3/CD28 mAbs [30]. Interestingly, levels of hyaluronidase 1 and -2 mRNAs in T cells from both SIs and MLNs were either undetectable or very low (as compared to levels of these mRNAs in other cell types), indicating that T cell-derived classical hyaluronidases are unlikely to be major factors in HA degradation.

Our observation that T cells can switch their expression of HAS mRNA between the HAS3 and HAS1/HAS2 isoforms (depending on tissue locale) is novel, as there are no previous reports of significant expression of HAS1 or HAS2 in T cells

or of HAS isoform switching in T cells – perhaps because previous studies of T cell-associated HASes were performed on cells isolated from lymphoid organs only, where HAS3 seems to prevail. In non-T cell types, environment-specific, differential regulation of HAS1 and HAS3 mRNAs has been reported. For example, in human synoviocyte cultures, transforming growth factor (TGF)-β strongly upregulates HAS1 mRNA, but suppresses HAS3 mRNA [31]. With respect to HAS2, elevated hexosamine biosynthesis associated with hyperglycemic environments leads to elevated transcription of HAS2 (but not HAS1 or -3) as a result of increased expression of the HAS2 natural antisense transcript HAS2-AS1 [32,33]. Collectively, a variety of studies demonstrate that regulation of the HAS isoforms is complex, operating at the transcriptional and post-translational levels via an interplay of metabolic pathways, growth factors, cytokines, and other signaling molecules [34]. In accordance with this theme, our future studies will attempt to identify locale-specific agents that contribute to HAS isoform switching by T cells.

The capability of T cells to express high levels of HAS1 mRNA (CN > 450) is remarkable. Of the three HAS isoforms, HAS1 has been studied the least – there have been relatively few reports on its regulation, potential function, and association with disease and only a single comprehensive review of the enzyme [35]. HAS1 is expressed by a variety of non-immune cell types (e.g., fibroblasts, synoviocytes, keratinocytes, vascular smooth muscle cells, and tumor cells) where it is upregulated by growth factors (e.g., TGF-β), pro-inflammatory cytokines such as tumor necrosis factor (TNF)-α and IL-1β [31,36–38], and prostaglandins [39]. In tissues, HAS1 is upregulated under conditions of inflammation, such as atherosclerosis, osteoarthritis, infectious lung disease, and dermal wound repair [35]. Compared to HAS2 and -3, HAS1 has a lower affinity for the HA synthetic substrates UDP-glucuronic acid and UDP-*N*-acetylglucosamine, which renders HA synthesis by HAS1 more susceptible to substrate availability [35,40]. In this context, the high CN of HAS1 mRNA in T cells might compensate for a relatively low rate of HA synthesis per HAS1 molecule. However, the production of HA-rich cell coats by HAS1-transfected MCF-7 cells is dramatically increased by high glucose media [38] suggesting that T1D-associated hyperglycemia could facilitate HA synthesis by HAS1.

Why T cells would use different HAS isoforms in different environments to produce HA is not known. Cell lines (COS-1, MCF-7) and primary arterial smooth muscle cells transfected to overexpress the three different HAS isoforms produce HA coats with distinctly different, isoform-specific densities and structures [35,41,42]. Accordingly, HAS isoform switching by T cells might allow the cells to tailor their HA coats to meet specific functional or environmental requirements in peripheral tissues vs. secondary lymphoid organs.

4MU is thought to inhibit HA synthesis by depleting cellular pools of UDP-glucuronic acid [43,44], which is accompanied by a reduction in expression of HAS mRNA in some cell types [45]. In animal models, 4MU suppresses inflammation and autoimmune disease in a variety of settings (reviewed by Nagy et al. [46]). In this context, we found that 4MU substantially suppressed infiltration of T cells (but not neutrophils or B cells) into SI allografts, which was accompanied by a lower level of T cell activation. Suppression was also observed in antigen-primed mice among $CD4^+$ T cells from secondary lymphoid organs, as indicated by a reduced antigen recall response and an increase in the proportion of $Foxp3^+$ regulatory T cells.

Studies in vitro have shown that mouse dendritic cells constitutively express HAS mRNA [25] and accumulate HA on their surfaces. Human dendritic cells are reported to express HA after exposure to activating cytokines (e.g., TNF-α, IL-2, and interferon-γ) and their binding to T cells is suppressed by pre-treatment of the dendritic cells with 50 μg/mL of 4MU [47]. Although these observations demonstrate a role for APC-derived HA in interactions between T cells and APCs, the present study indicates that T cell activation is also influenced by T cell-derived HA. We observed that CD69 upregulation by DO11.10 T cells 24 h after co-culture with APCs and OVA peptide was inhibited by pre-exposure of the T cells to 20–100 μg/mL of 4MU, but was not inhibited by pre-exposure of the APCs to 4MU. Interestingly, somewhat different results with respect to CD69 expression were reported by Mahaffey and Mummert [26], who observed that while 4MU at 100 μg/mL inhibited HA production and proliferation of T cells in vitro in response to activation by ConA, 4MU did not inhibit CD69 upregulation 24 h after this activation. This discrepancy with our observations might reflect differences in the choice of activation agent (i.e., ConA vs. APC-mediated stimulation of the TcR by OVA peptide) and suggests that specific components of the T cell activation process might be differentially influenced by T cell-derived HA. This notion is underscored by our findings that suggest a role for T cell-derived HA at different points of the T cell activation timeline, including early (CD3ζ phosphorylation) and downstream (CD69 expression) events.

Collectively, our observations that: 1) inhibition of HA synthesis suppresses T cell auto- (and allo-) immune responses in vivo, 2) there are robust changes in expression levels of HAS1–3 mRNAs by T cells in peripheral tissue vs. secondary lymphoid organs, and 3) there is direct involvement of T cell-derived HA in T cell signaling and activation, support the idea that production of this extracellular matrix molecule *by T cells themselves* might be critical to T cell function. Our future studies will continue to explore the roles of T cell-derived HA in autoimmunity.

Experimental procedures

Mouse models

One day after implantation of SIs containing RIP-mOVA islets into RIP-mOVA/Rag2$^{-/-}$ mice, OVA-directed immune responses were initiated in the mice by a retro-orbital injection (under isoflurane anesthesia) of 100 µL of PBS containing 1×10^5 CD3$^+$/CD4$^+$ T cells from transgenic DO11.10/Rag2$^{-/-}$ mice (isolated from mixed splenocytic and LN suspensions by magnetic column, Product 130-104-454, MiltenyiBiotec Inc., Auburn, CA). One day after T cell transfer, the mice were given a subcutaneous injection of 100 µg of $OVA_{323–339}$ peptide (Product 27025, AnaSpec Inc., Fremont, CA) in incomplete Freund's adjuvant to prime the immune system. Additional experiments utilized islet allotransplants – SIs loaded with BALB/c mouse islets were transplanted into C57BL/6 mice.

To evaluate the effects of systemic inhibition of HA synthesis on T cell behavior in vivo, mice were fed with mouse chow supplemented with 5% 4MU by weight (TestDiet, St. Louis, MO) [18,48], or the same formulation of chow lacking 4MU (control chow) for 2 to 6 weeks prior to the start of experiments.

All work with mice was performed in the Benaroya Research Institute vivarum under a protocol approved by the Benaroya Research Institute Animal Care and Use Committee. This vivarium is accredited by the Association for Assessment and Accreditation of Laboratory Animal Care (AAALAC) International.

Isolation of islets

Islets for transplantion were isolated from 12 to 24-week-old RIP-mOVA/Rag2$^{-/-}$ or standard BALB/c mice by digestion of the pancreata with collagenase P (Product 11249002001, Roche Diagnostics, Indianapolis, IN) and centrifugation of the digests through a culture medium-Histopaque®-1077 (MilliporeSigma, Burlington, MA) interface, as described previously [22–24]. Immediately after all islets were isolated, they were hand-picked once, cultured overnight in an incubator (37 °C/5% CO_2/100% humidity), and then hand-picked a second time. Yields averaged 125–175 islets per mouse. Total time of islet culture (i.e., from isolation to surgical implantation) was approximately 24 h.

Fabrication of PVA scaffolds for SIs

Biopsy punches (Sklar Surgical Instruments, West Chester, PA) were used to cut 8-mm diameter disks from 2-mm thick sheets of medical-grade Merocel® CF90 PVA sponge (500 µm average pore size with no surfactant treatment – a generous gift from Merocel/Medtronic, Inc., Minneapolis, MN). Subsequently, each disk was through-punched with five, 2-mm diameter holes (chambers) in a pentagonal pattern. The punched disks were washed on a rocker in 50 mL centrifuge tubes filled with 40 mL of sterile distilled water (10 min per wash, repeated five times), then air-dried on sterile gauze, transferred to 60-mm petri dishes, exposed to γ-irradiation, and stored until needed for SI assembly.

Preparation of type I collagen solution for SIs

One volume of a stock solution of rat tail native type I collagen in dilute acetic acid (Product 354236, Corning/Discovery Labware, Bedford, MA) was combined with 1/9 volume of 10-strength Medium 199 (Gibco/ThermoFisher, Waltham, MA) saturated with $NaHCO_3$, and sufficient Dulbecco's Modified Eagle Medium (DMEM; Gibco), normal mouse serum (NMS), and 1 N NaOH to yield a pH 7.4 solution containing 2.5 mg/mL collagen and 10% NMS [22,49]. The collagen solution was prepared just prior to SI assembly and maintained on ice until needed.

Assembly of SIs

Dry PVA sponge scaffolds were expanded for 5 min in sterile, deionized water, then blotted on sterile gauze, transferred to inverted 60-mm plastic tissue culture dish tops lined with UV-sterilized hydrophobic Parafilm™ "M" (Pechiney Plastic Packaging, Chicago, IL), and infused with 75 µL of type I collagen solution containing suspended islets. Within a given experiment, each SI received an identical number of islets (approximately 250). The PVA sponge absorbed the collagen solution, with the majority of the islets entering the five, 2-mm diameter chambers. Subsequently, the dish tops were covered with 60-mm dish bottoms that were lined with moist filter paper and incubated for 30 min at 37 °C/5% CO_2/100% humidity to gel the collagen. The completed SIs were transferred to a 24-well tissue culture plate filled with 500 µL/well of pre-equilibrated DMEM supplemented with 10% NMS and 100 µg/mL penicillin/100 U/mL streptomycin (pen/strep), and maintained briefly in a tissue culture incubator prior to implantation into mice.

Implantation of SIs

Recipient mice were given buprenorphine (0.05–0.1 mg/kg) 30 min prior to surgery, which was performed under isoflurane. A 1-cm vertical, mid-line incision was made in the skin and peritoneum, a loop of the small intestine was extracted, and the SI placed on the intestinal mesentery [22,24]. Subsequently, the intestinal loop was folded over the SI and returned to the peritoneal cavity. The incision was closed with absorbable sutures for the peritoneum and staples for the skin. A subcutaneous

injection of meloxicam (5 mg/kg) was administered immediately after surgery and additional analgesics (buprenorphine) were given as needed. Blood glucose levels of RIP-mOVA mice that received transplanted islets were monitored daily as described previously [22–24]. The mice were euthanized and SIs removed after 13 days, a time when blood glucose levels exceeded 250 mg/dL, which indicated that autoimmune destruction of both native and transplanted islets was fully underway. C57BL/6 mice that received BALB/c islet allotransplants in SIs were euthanized and the SIs removed after 7 or 14 days, times representing a well-developed rejection response to the transplanted islets.

AHC/IHC analyses

SIs were explanted and fixed in 10% neutral-buffered formalin, dehydrated, embedded in paraffin, and sectioned at 8 μm *en face* across the entire diameter of the SI disk. Sections were deparaffinized, blocked in PBS/2% normal goat serum, and exposed overnight to PBS/2% normal goat serum containing 5 μg/mL of primary mAbs or polyclonal antibodies (pAbs) identifying mouse T cells (rabbit anti-CD3 mAb SP7, Product ab16669, Abcam, San Francisco, CA), B cells (rat anti-B220 mAb RA3-6B2, Product ab64100, Abcam), and neutrophils (rabbit anti-myeloperoxidase pAb, Product ab9535, Abcam). In selected experiments, anti-CD3 mAb-stained specimens were also stained with rabbit pAbs to HAS1 or HAS2 (Products 5-50674 and 5-25593, ThermoFisher). Bound primary Abs were visualized with goat anti-rabbit or anti-rat secondary Abs conjugated to Alexa-Fluor 488 or -546 (ThermoFisher). HA in the sections was labeled by AHC with biotinylated HABP (bHABP, Product 385911, Calbiochem®/MilliporeSigma) in conjunction with Alexa-Fluor 488-streptavidin (ThermoFisher). Images were recorded with a Leica TCS SP5 II scanning confocal microscope. In conjunction with AHC/IHC staining, islets were identified in confocal views of sections by use of differential interference contrast optics. The appearance of islets is quite distinctive using this viewing mode.

To quantify infiltration of cells into SIs using IHC, sections were labeled with a single Ab recognizing either T cells, B cells, or neutrophils, as described above. For each cell type, six sections (each separated by 100 μm) were evaluated for each SI. Each entire section was imaged by collecting 40–50 digital images with a 20× objective (each image covered a 1 mm^2 field) and the total number of each cell type present in the total cellularized area of the section was determined (the cellularized areas occupied the chambers, pores, and pore throats of the sponge – the acellular areas occupied by the PVA sponge proper were not included). Results were recorded as average cell number per mm^2 of cellularized area. Data were collected from three mice each within the control and 4MU-fed groups.

Isolation of cellular infiltrates from SIs and analytical flow cytometry

Cellular infiltrates were removed from explanted SIs by incubating each SI in a covered 60-mm tissue culture dish containing 2 mL of 37 °C "DMEM-10" (DMEM supplemented with 10% fetal bovine serum, 50 μM 2-mercaptoethanol, 2 mM glutamine, 1 mM sodium pyruvate, and pen/strep) containing 1 mg/mL collagenase P. During the incubation, the dishes were swirled gently in a 37 °C water bath and the sponge scaffolds of the SIs were squeezed at 10 min intervals with a sterile, 1 mL syringe plunger to expel all of the infiltrating cells. The expelled cells were centrifuged for 10 min at 270 × *g* and then incubated for 5 min in 1 mL of 37 °C ammonium chloride/potassium (ACK) buffer [50] to lyse red blood cells.

For flow cytometry, 1–5 × 10^6 cells were incubated 15 min on ice in 50 μL of "stain buffer" (PBS, 2% fetal bovine serum, 0.05% NaN_3) containing 2 μg of Fc-blocking mAb 2.4G2 (Mouse BD Fc Block™, Product 553141, BD Biosciences, San Jose, CA). Subsequently, a 50 μL mixture of chromophore-tagged mAbs was added and incubated for an additional 30 min on ice. The mixture included mAbs 145-2C11, RM4-5, M5/114.15.2 and H1.2F3 (BioLegend/ThermoFisher) recognizing CD3, CD4, MHC class II, and CD69, respectively. Cells were washed with 1 mL of stain buffer and then labeled for nuclear Foxp3 using a Foxp3 staining buffer kit (Product 00-5523-00, eBioscience/ThermoFisher) with anti-Foxp3 mAb FJK-16s (eBioscience/ThermoFisher). Samples were fixed with 2% formaldehyde in PBS, run on an LSR II flow cytometer (BD Biosciences), and analyzed with FlowJo cytometric software (FlowJo LLC, Ashland, OR).

In vitro T cell proliferation assays

To assess DO11.10 T cell antigen recall (proliferation) in vitro, mice were immunized at the base of the tail by a subcutaneous injection of 50 μg of OVA peptide in 100 μL of 50% incomplete Freund's adjuvant (Product A7642, MilliporeSigma) in PBS. Two weeks later, the ILNs and spleens were explanted and the cells isolated by gently pressing the tissue through 40 μm cell strainers (Product 22363547, ThermoFisher). LN cells were washed in DMEM-10. Splenocytes were exposed to ACK buffer to lyse red blood cells prior to resuspension in DMEM-10. For assays, 1 × 10^5 LN cells or 5 × 10^5 splenocytes were plated in round-bottom 96-well plates in 150 μL of DMEM-10 containing graded concentrations of OVA peptide (0–5 μg/mL) or a mixture of 2 μg/mL of anti-CD3 mAb 145-2C11 and

0.4 μg/mL of anti-CD28 mAb 37.51 (eBioscience/ThermoFisher). After 72 h of culture, 1 μCi of [^{3}H]-thymidine (Moravek Inc., Brea, CA) was added to each well in 25 μL of DMEM-10 and incorporation of the radiolabel measured 24 h later with a 1450 Microbeta® TriLux microplate scintillation counter (Wallac-PerkinElmer Inc., Waltham, MA).

Allo-MLR assays were performed in flat-bottomed 96-well plates to assess T cell alloantigen recall (proliferation) in vitro. Splenocytes (5×10^5) from C57BL/6 mice transplanted with BALB/c islets were isolated and co-cultured for 84 h with 5×10^5 irradiated BALB/c splenocytes (3000 rads from ^{137}Cs). Subsequently, the cultures received [^{3}H]-thymidine and incorporation of the radiolabel measured 24 h later.

To evaluate the involvement of HA associated with either T cells or APCs in T cell activation, DO11.10 CD4$^+$ T cells and MHC class II$^+$ APCs were isolated from combined spleen and LN suspensions using magnetic columns (Products 130-104-454 and 130-052-401, MiltenyiBiotec Inc.) and separately cultured for 24 h in the presence of 4MU at 0, 20, 50, or 100 μg/mL. Subsequently, the T cells and APCs were washed in DMEM-10 and co-cultured in the presence of OVA peptide at 0, 0.8, 4, or 20 μg/mL. After 24 h of OVA stimulation, expression of the early activation marker CD69 on CD3$^+$/CD4$^+$/CD44^{med} gated cells was determined by flow cytometry.

mRNA analyses

Infiltrating cells removed from explanted SIs were first enriched for CD4$^+$ T cells using magnetic columns as described above. Cells were then flow-sorted on a FACS Aria II to obtain a high-purity T cell (CD3$^+$/CD4$^+$/MHC class II$^-$) fraction. To preserve cell integrity, cells were suspended in DMEM for FACS staining and sorting. The isolated T cells ($50–200 \times 10^3$) were lysed in 0.5 mL TRIzol® Reagent (ThermoFisher) followed by the addition of 0.1 mL chloroform and vigorous mixing. The solution was incubated at room temperature for 5 min and spun at 14,000 × *g* for 10 min at 4 °C. The aqueous phase was collected, mixed with an equal volume of 70% ethanol, and purified using EconoSpin™ columns (Epoch Life Science, Missouri City, TX). cDNA was prepared from the isolated RNA with a High Capacity cDNA Reverse Transcription Kit (ThermoFisher) according to the manufacturer's instructions. Real-time PCR was carried out with SYBR Select Master Mix or TaqMan® Gene Expression Master Mix (ThermoFisher), as directed by the manufacturer, on an Applied Biosystems 7900HT Fast Real-Time PCR System. For each sample, assays were run as technical duplicates. cDNA levels were then expressed as estimated CN of mRNA relative to 10^5 18S rRNA using the master-template approach [51]. Taqman probes (ThermoFisher) were for murine HAS1 (Mm00468496_m1), HAS2 (Mm00515089_m1), HAS3 (Mm00515092_m1), hyaluronidase 1 (Mm00476206_m1), hyaluronidase 2 (Mm01230689_g1), and 18S rRNA (Product 4318839). Identical assays were performed on T cells isolated from MLNs.

Assessment of HA on the T cell surface

Naïve splenic DO11.10 CD4$^+$ T cells were isolated by magnetic column and stimulated for 3–4 days in DMEM-10 containing anti-CD3/CD28 mAbs at 2/0.4 μg/mL. To demonstrate presence of cell surface HA, T cells were labeled for 1 h at 4 °C with bHABP (10 μg/mL) and Fc-Block (10 μg/mL), washed, stained with streptavidin-phycoerythrin (SA-PE, Product 12-4317-87, eBioscience/ThermoFisher) and allophycocyanin-tagged anti-CD4 mAb (clone RM4-5, eBioscience/ThermoFisher), and analyzed on a FACS Caliber flow cytometer. Controls consisted of cells exposed to SA-PE only, or no stain. The effect of hyaluronidase digestion on expression of HA by 3-day cultures of anti-CD3/CD28 mAb-activated T cells was examined by a 2-h, 37 °C incubation of the cells in 20 U/mL of *Streptomyces hyalurolyticus* hyaluronidase (Product H1136, Millipore-Sigma) added directly to the culture medium, followed by a washing step and bHABP/SA-PE flow cytometry as described above. The effect of 4MU on HA expression was evaluated by culturing the T cells for 4 days in anti-CD3/CD28 mAb activation medium supplemented with 100 μg/mL of 4MU on day 1 (for a 96-h exposure), or day 3 (for a 24-h exposure). Cells cultured 4 days in activation medium lacking 4MU served as controls.

In vitro T cell signaling assays

To determine the effects of pre-exposure of T cells to 4MU on early signaling in the TcR, naïve DO11.10 CD4$^+$ T cells (isolated by magnetic column and checked for purity and viability by flow cytometry) were separately cultured for 20 h with or without 100 μg/mL of 4MU, washed, allowed to rest for 1 h in 4MU-free medium, and then stimulated for 5 min with anti-CD3/CD28 mAbs at 2/0.4 μg/mL. Stimulation was immediately followed by fixation and permeabilization (Intracellular Fixation & Permeabilization Buffer Set, Product 88-8824-00, eBioscience/ThermoFisher), labeling with mAbs against CD4 (clone RM4-5) and phospho- (p)CD3ζ (clone K25-407.69, BD Biosciences), and analysis by flow cytometry [29].

Statistical analyses

P values were calculated with Prism® (GraphPad Software, Inc.) using two-tailed *t*-tests (unpaired or paired, as applicable).

Abbreviations

4MU	4-methylumbelliferone
AHC	affinity histochemistry
APC	antigen-presenting cell
bHABP	biotinylated hyaluronan binding protein
CN	copy number
FFPE	formalin-fixed/paraffin-embedded
HA	hyaluronan
HAS	hyaluronan synthase
IHC	immunohistochemistry
ILNs and MLNs	inguinal and mesenteric lymph nodes
MLR	mixed lymphocyte reaction
OVA	ovalbumin
PVA	polyvinyl alcohol
SI	scaffolded islet implant
T1D	type 1 diabetes
TcR	T cell receptor

CRediT authorship contribution statement

Research design, J.A.G, R.B.V.; research performance, J.A.G., M.D.G., G.W., R.B.V.; ideation, J.A.G., N.N., P.L.B., T.N.W., R.B.V.; manuscript writing/project management, R.B.V.

Declaration of competing interest

The authors declare no conflicts of interest.

Acknowledgements

The authors thank Pamela Y. Johnson, Ph.D. of the Benaroya Research Institute Histology/Imaging Core for histological preparation of samples and Virginia M. Green, Ph.D. for editorial assistance. This project was supported by a major grant from the Klorfine Foundation (R.B.V.), a Commercialization Gap Funding Program grant from the Benaroya Research Institute (T.N.W., J.A.G.), and NIH R01 DK096087 (P.L.B.). The funding sources had no involvement in study design; in the collection, analysis and interpretation of data; in the writing of this article; or in the decision to submit this article for publication.

Received 22 May 2019;
Received in revised form 11 November 2020;
Accepted 11 November 2020
Available online 30 December 2020

Keywords:
4-methylumbelliferone;
Hyaluronan synthases;
Implant;
Mouse;
T cell;
Type 1 diabetes

References

[1] M.I. Tammi, A.J. Day, E.A. Turley, Hyaluronan and homeostasis: a balancing act, J. Biol. Chem. 277 (2002) 4581–4584.
[2] N.K. Karamanos, Z. Piperigkou, A.D. Theocharis, H. Watanabe, M. Franchi, S. Baud, S. Brezillon, M. Gotte, A. Passi, D. Vigetti, S. Ricard-Blum, R.D. Sanderson, T. Neill, R.V. Iozzo, Proteoglycan chemical diversity drives multifunctional cell regulation and therapeutics, Chem. Rev. 118 (2018) 9152–9232.
[3] A.J. Day, C.A. de la Motte, Hyaluronan cross-linking: a protective mechanism in inflammation? Trends Immunol. 26 (2005) 637–643.
[4] S. Garantziotis, R.C. Savani, Hyaluronan biology: a complex balancing act of structure, function, location and context, Matrix Biol. 78-79 (2019) 1–10.
[5] A.J. Day, C.M. Milner, TSG-6: a multifunctional protein with anti-inflammatory and tissue-protective properties, Matrix Biol. 78-79 (2019) 60–83.
[6] B.P. Toole, T.N. Wight, M.I. Tammi, Hyaluronan-cell interactions in cancer and vascular disease, J. Biol. Chem. 277 (2002) 4593–4596.
[7] D. Jiang, J. Liang, P.W. Noble, Hyaluronan as an immune regulator in human diseases, Physiol. Rev. 91 (2011) 221–264.
[8] R.H. Tammi, A.G. Passi, K. Rilla, E. Karousou, D. Vigetti, K. Makkonen, M.I. Tammi, Transcriptional and post-translational regulation of hyaluronan synthesis, FEBS J. 278 (2011) 1419–1428.
[9] S.M. Ruppert, T.R. Hawn, A. Arrigoni, T.N. Wight, P.L. Bollyky, Tissue integrity signals communicated by high-molecular weight hyaluronan and the resolution of inflammation, Immunol. Res. 58 (2014) 186–192.
[10] J.M. Delmage, D.R. Powars, P.K. Jaynes, S.E. Allerton, The selective suppression of immunogenicity by hyaluronic acid, Ann. Clin. Lab. Sci. 16 (1986) 303–310.
[11] R. Stern, M.J. Jedrzejas, Hyaluronidases: their genomics, structures, and mechanisms of action, Chem. Rev. 106 (2006) 818–839.
[12] J.D. Powell, M.R. Horton, Threat matrix: low-molecular-weight hyaluronan (HA) as a danger signal, Immunol. Res. 31 (2005) 207–218.
[13] S.S. Lee-Sayer, Y. Dong, A.A. Arif, M. Olsson, K.L. Brown, P. Johnson, The where, when, how, and why of hyaluronan binding by immune cells, Front. Immunol. 6 (2015) 150.
[14] N. Nagy, H.F. Kuipers, P.L. Marshall, E. Wang, G. Kaber, P.L. Bollyky, Hyaluronan in immune dysregulation and autoimmune diseases, Matrix Biol. 78-79 (2019) 292–313.
[15] R.L. Hull, P.Y. Johnson, K.R. Braun, A.J. Day, T.N. Wight, Hyaluronan and hyaluronan binding proteins are normal components of mouse pancreatic islets and are differentially

expressed by islet endocrine cell types, J. Histochem. Cytochem. 60 (2012) 749–760.
[16] M. Bogdani, P.Y. Johnson, S. Potter-Perigo, N. Nagy, A.J. Day, P.L. Bollyky, T.N. Wight, Hyaluronan and hyaluronan-binding proteins accumulate in both human type 1 diabetic islets and lymphoid tissues and associate with inflammatory cells in insulitis, Diabetes 63 (2014) 2727–2743.
[17] M. Bogdani, E. Korpos, C.J. Simeonovic, C.R. Parish, L. Sorokin, T.N. Wight, Extracellular matrix components in the pathogenesis of type 1 diabetes, Curr Diab Rep 14 (2014) 552.
[18] N. Nagy, G. Kaber, P. Johnson, J. Gebe, A. Preisinger, B. Falk, V. Sunkari, M. Gooden, R. Vernon, M. Bogdani, H. Kuipers, A. Day, D. Campbell, T. Wight, P. Bollyky, Inhibition of hyaluronan synthesis restores immune tolerance during autoimmune insulitis, J. Clin. Invest. 185 (2015) 372–381.
[19] B.O. Roep, I. Stobbe, G. Duinkerken, J.J. van Rood, A. Lernmark, B. Keymeulen, D. Pipeleers, F.H. Claas, R.R. de Vries, Auto- and alloimmune reactivity to human islet allografts transplanted into type 1 diabetic patients, Diabetes 48 (1999) 484–490.
[20] P. Monti, M. Scirpoli, P. Maffi, N. Ghidoli, F. De Taddeo, F. Bertuzzi, L. Piemonti, M. Falcone, A. Secchi, E. Bonifacio, Islet transplantation in patients with autoimmune diabetes induces homeostatic cytokines that expand autoreactive memory T cells, J. Clin. Invest. 118 (2008) 1806–1814.
[21] T.L. van Belle, K.T. Coppieters, M.G. von Herrath, Type 1 diabetes: etiology, immunology, and therapeutic strategies, Physiol. Rev. 91 (2011) 79–118.
[22] R.B. Vernon, A. Preisinger, M.D. Gooden, L.A. D'Amico, B. B. Yue, P.L. Bollyky, C.S. Kuhr, T.R. Hefty, G.T. Nepom, J.A. Gebe, Reversal of diabetes in mice with a bioengineered islet implant incorporating a type I collagen hydrogel and sustained release of vascular endothelial growth factor, Cell Transplant. 21 (2012) 2099–2110.
[23] J.A. Gebe, A. Preisinger, M.D. Gooden, L.A. D'Amico, R.B. Vernon, Local, controlled release in vivo of vascular endothelial growth factor within a subcutaneous scaffolded islet implant reduces early islet necrosis and improves performance of the graft, Cell Transplant. 27 (2018) 531–541.
[24] R.B. Vernon, M.D. Gooden, A. Preisinger, J.A. Gebe, Controlled release of monoclonal antibodies from poly-l-lysine-coated alginate spheres within a scaffolded implant mitigates autoimmune responses to transplanted islets and limits systemic antibody toxicity, Mater. Sci. Eng. C Mater. Biol. Appl. 93 (2018) 390–398.
[25] M.E. Mummert, D. Mummert, D. Edelbaum, F. Hui, H. Matsue, A. Takashima, Synthesis and surface expression of hyaluronan by dendritic cells and its potential role in antigen presentation, J. Immunol. 169 (2002) 4322–4331.
[26] C.L. Mahaffey, M.E. Mummert, Hyaluronan synthesis is required for IL-2-mediated T cell proliferation, J. Immunol. 179 (2007) 8191–8199.
[27] L.J. Thompson, A.C. Valladao, S.F. Ziegler, Cutting edge: De novo induction of functional Foxp3+ regulatory CD4 T cells in response to tissue-restricted self antigen, J. Immunol. 186 (2011) 4551–4555.
[28] C. Kurts, W.R. Heath, F.R. Carbone, J. Allison, J.F. Miller, H. Kosaka, Constitutive class I-restricted exogenous presentation of self antigens in vivo, J. Exp. Med. 184 (1996) 923–930.
[29] R. Uzana, G. Eisenberg, Y. Sagi, S. Frankenburg, S. Merims, N. Amariglio, E. Yefenof, T. Peretz, A. Machlenkin, M. Lotem, Trogocytosis is a gateway to characterize functional diversity in melanoma-specific CD8+ T cell clones, J. Immunol. 188 (2012) 632–640.
[30] S. Homann, M. Grandoch, L.S. Kiene, Y. Podsvyadek, K. Feldmann, B. Rabausch, N. Nagy, S. Lehr, I. Kretschmer, A. Oberhuber, P. Bollyky, J.W. Fischer, Hyaluronan synthase 3 promotes plaque inflammation and atheroprogression, Matrix Biol. 66 (2018) 67–80.
[31] K.M. Stuhlmeier, C. Pollaschek, Differential effect of transforming growth factor beta (TGF-beta) on the genes encoding hyaluronan synthases and utilization of the p38 MAPK pathway in TGF-beta-induced hyaluronan synthase 1 activation, J. Biol. Chem. 279 (2004) 8753–8760.
[32] D. Vigetti, S. Deleonibus, P. Moretto, T. Bowen, J.W. Fischer, M. Grandoch, A. Oberhuber, D.C. Love, J.A. Hanover, R. Cinquetti, E. Karousou, M. Viola, M.L. D'Angelo, V.C. Hascall, G. De Luca, A. Passi, Natural antisense transcript for hyaluronan synthase 2 (HAS2-AS1) induces transcription of HAS2 via protein O-GlcNAcylation, J. Biol. Chem. 289 (2014) 28816–28826.
[33] P. Moretto, E. Karousou, M. Viola, I. Caon, M.L. D'Angelo, G. De Luca, A. Passi, D. Vigetti, Regulation of hyaluronan synthesis in vascular diseases and diabetes, J. Diabetes Res. 2015 (2015) 167283.
[34] P. Heldin, C.Y. Lin, C. Kolliopoulos, Y.H. Chen, S.S. Skandalis, Regulation of hyaluronan biosynthesis and clinical impact of excessive hyaluronan production, Matrix Biol. 78-79 (2019) 100–117.
[35] H. Siiskonen, S. Oikari, S. Pasonen-Seppanen, K. Rilla, Hyaluronan synthase 1: a mysterious enzyme with unexpected functions, Front. Immunol. 6 (2015) 43.
[36] Y. Yamada, N. Itano, K. Hata, M. Ueda, K. Kimata, Differential regulation by IL-1beta and EGF of expression of three different hyaluronan synthases in oral mucosal epithelial cells and fibroblasts and dermal fibroblasts: quantitative analysis using real-time RT-PCR, J Invest Dermatol 122 (2004) 631–639.
[37] T. Oguchi, N. Ishiguro, Differential stimulation of three forms of hyaluronan synthase by TGF-beta, IL-1beta, and TNF-alpha, Connect. Tissue Res. 45 (2004) 197–205.
[38] H. Siiskonen, R. Karna, J.M. Hyttinen, R.H. Tammi, M.I. Tammi, K. Rilla, Hyaluronan synthase 1 (HAS1) produces a cytokine-and glucose-inducible, CD44-dependent cell surface coat, Exp. Cell Res. 320 (2014) 153–163.
[39] J.W. Fischer, K. Schror, Regulation of hyaluronan synthesis by vasodilatory prostaglandins. Implications for atherosclerosis, Thromb. Haemost. 98 (2007) 287–295.
[40] N. Itano, T. Sawai, M. Yoshida, P. Lenas, Y. Yamada, M. Imagawa, T. Shinomura, M. Hamaguchi, Y. Yoshida, Y. Ohnuki, S. Miyauchi, A.P. Spicer, J.A. McDonald, K. Kimata, Three isoforms of mammalian hyaluronan synthases have distinct enzymatic properties, J. Biol. Chem. 274 (1999) 25085–25092.
[41] T.S. Wilkinson, S.L. Bressler, S.P. Evanko, K.R. Braun, T.N. Wight, Overexpression of hyaluronan synthases alters vascular smooth muscle cell phenotype and promotes monocyte adhesion, J. Cell. Physiol. 206 (2006) 378–385.
[42] K. Rilla, S. Oikari, T.A. Jokela, J.M. Hyttinen, R. Karna, R.H. Tammi, M.I. Tammi, Hyaluronan synthase 1 (HAS1) requires higher cellular UDP-GlcNAc concentration than HAS2 and HAS3, J. Biol. Chem. 288 (2013) 5973–5983.
[43] T.A. Jokela, M. Jauhiainen, S. Auriola, M. Kauhanen, R. Tiihonen, M.I. Tammi, R.H. Tammi, Mannose inhibits hyaluronan synthesis by down-regulation of the cellular pool of UDP-N-acetylhexosamines, J. Biol. Chem. 283 (2008) 7666–7673.
[44] I. Kakizaki, K. Kojima, K. Takagaki, M. Endo, R. Kannagi, M. Ito, Y. Maruo, H. Sato, T. Yasuda, S. Mita, K. Kimata, N.

Itano, A novel mechanism for the inhibition of hyaluronan biosynthesis by 4-methylumbelliferone, J. Biol. Chem. 279 (2004) 33281–33289.

[45] A. Kultti, S. Pasonen-Seppanen, M. Jauhiainen, K.J. Rilla, R. Karna, E. Pyoria, R.H. Tammi, M.I. Tammi, 4-Methylumbelliferone inhibits hyaluronan synthesis by depletion of cellular UDP-glucuronic acid and downregulation of hyaluronan synthase 2 and 3, Exp. Cell Res. 315 (2009) 1914–1923.

[46] N. Nagy, H.F. Kuipers, A.R. Frymoyer, H.D. Ishak, J.B. Bollyky, T.N. Wight, P.L. Bollyky, 4-methylumbelliferone treatment and hyaluronan inhibition as a therapeutic strategy in inflammation, autoimmunity, and cancer, Front. Immunol. 6 (2015) 123, https://doi.org/10.3389/fimmu.2015.00123.

[47] P.L. Bollyky, S.P. Evanko, R.P. Wu, S. Potter-Perigo, S.A. Long, B. Kinsella, H. Reijonen, K. Guebtner, B. Teng, C.K. Chan, K.R. Braun, J.A. Gebe, G.T. Nepom, T.N. Wight, Th1 cytokines promote T-cell binding to antigen-presenting cells via enhanced hyaluronan production and accumulation at the immune synapse, Cell Mol Immunol 7 (2010) 211–220.

[48] N. Nagy, T. Freudenberger, A. Melchior-Becker, K. Rock, M. Ter Braak, H. Jastrow, M. Kinzig, S. Lucke, T. Suvorava, G. Kojda, A.A. Weber, F. Sorgel, B. Levkau, S. Ergun, J.W. Fischer, Inhibition of hyaluronan synthesis accelerates murine atherosclerosis: novel insights into the role of hyaluronan synthesis, Circulation 122 (2010) 2313–2322.

[49] R.B. Vernon, M.D. Gooden, New technologies in vitro for analysis of cell movement on or within collagen gels, Matrix Biol. 21 (2002) 661–669.

[50] A.M. Kruisbeek, Isolation of mouse mononuclear cells, Curr Protoc Immunol (2001) Chapter 3. Unit 3.1.

[51] S.C. Shih, L.E. Smith, Quantitative multi-gene transcriptional profiling using real-time PCR with a master template, Exp. Mol. Pathol. 79 (2005) 14–22.